Sensors & Transducers, Vol. 24, Special Issue, August 2013, pp. 7-18

www.sensorsportal.com

Sensors & Transducers

http://www.sensorsportal.com

Versatile Signal Acquisition System for Ultrasound Equipment Frequency Domain Parameters Estimation

Linas SVILAINIS, Vytautas DUMBRAVA, Andrius CHAZIACHMETOVAS

Signal Processing Department, Kaunas University of Technology,
Studentu str. 50-340, Kaunas, LT-51368, Lithuania
Tel.: +370-37-300532
E-mail: linas.svilainis@ktu.lt

Received: 15 May 2013 /Accepted: 16 August 2013 /Published: 30 August 2013

Abstract: Versatile system for ultrasound equipment parameters measurement is presented. The system is based on single direct digital synthesis (DDS) generator which is used for excitation and dual simultaneous sampling analog-to-digit (ADC) conversion channels. System is dedicated for ultrasound equipment frequency domain parameters measurement: transduction AC response, insertion loss AC response, harmonic distortion, noise and electrical impedance can be estimated. Since primary application of the system is the ultrasonic equipment performance evaluation, operating frequencies range corresponds to most common ultrasound frequencies. Frequency range 20 kHz to 30 MHz was targeted. Despite being aimed for parameters comparison and estimation, system is universal: several measurements can be arranged using one excitation and two reception channels. System structure and setups for the aforementioned measurements are presented. Modular PC104 form-factor construction allows operating the system in both local and remote PC connectivity mode. Setup for most common tasks and examples of measurement results obtained are presented.

Keywords: Acquisition system, Gain AC response, Ultrasound transmission measurement, Noise measurement, Sine wave correlation, Impedance measurement, Distortion measurement, Power delivery efficiency.

1. Introduction

There is a need for ultrasonic equipment parameters estimation, verification or comparison [1], while designing or setting the ultrasonic system for experiment. Usually the variation in frequency domain is one of the essential parameters being investigated [2]. Sometimes just single frequency gain value is enough, but there is a need to adjust that frequency value. Parameters that are most frequently evaluated [3] are gain or transmission AC response, impedance, signal distortion and noise. Several new parameters can be rectified: input referred noise can be obtained from output noise and gain AC response values [4]; noise figure [5]; power delivery to load efficiency [6] and expected noise level [7] can be obtained from measured ultrasonic transducer impedance. It is useful to have the frequency domain parameters monitoring of the device during the design process iterations or while in service.

Therefore we indicate the need for versatile measurement system [1], capable to perform the most common measurement tasks: vector voltage, impedance, noise power spectral density, transmission. We put the versatility of the system in

front of accuracy and reliability of measurements. Ultrasonic equipment AC parameter evaluation is aimed. Therefore frequency range was defined by the target: 20 kHz to 30 MHz. System should be able to measure the complex transmission AC response, signal distortion, noise and impedance of the device under test (DUT). Measurements should be collectable on host PC for further processing and storage.

Three approaches are available here:

i) Collect a set of bench top equipment: network analyzer, spectrum analyzer, impedance analyzer, digital storage oscilloscope;

ii) Use a commercially available data acquisition system and design additional modules for impedance measurement, high impedance input;

iii) Build a dedicated system, capable of all the aforementioned tasks.

Though i) approach seems most simple and essential it requires large investment and take significant place on a bench. Approach iii) is not attractive since significant effort and expertise has to be put to make sure no parts are missed. Approach ii) seems the easiest one. Such systems can be divided into 2 parts: small, inexpensive units with USB connectivity to local host or VXI bus architecture or other standard bus modular systems [8]. While modular systems are attractive (they can be operated both remote or locally) they are expensive and also have large footprint. We decided to use the mixture of ii) and iii): we build a modular system with possibility for expansion, flexibility of control host location and advantage of small size. Instead of using a commercially available system, we designed our own system, based on PC104 size and bus. Requirements for ADC and DDS blocks were rectified first. Brief presentation of material was given in [1]. Here we present the expanded version of research: details on device design and the system application examples.

2. Voltage Vector Estimation Using Sine Wave Correlation

We assume that the frequency response at certain frequency is determined by probing the system input with a single frequency continuous wave (CW) signal while measuring the input/output amplitude ratio and phase difference. By experience we know that electromagnetic interference or other sources on noise may exist in measured system due to several reasons: sensitivity usually is high; measured objects sometimes are taken out of their corresponding shielding; out-of-band transmission is sometimes required; material attenuation can be high etc. Then, presence of the noise turns the amplitude and phase estimation into more difficult task. Narrowband filtering can address the problem. It is interesting to point out that several advantages are obtained if filtering is done in software: stability of filter parameter, ability to control phase response, reduced demands for dynamic range of the acquisition channel. Several techniques for vector voltage estimation exist: sine fitting using the least squares error techniques [9], Fourier transform, interpolated discrete Fourier transform, short-time Fourier Transform [10-12] or wavelet transform [13] are used for parameter estimation. These techniques are used if the sine frequency is not known or the sampling frequency value is not as accurate as would be expected. The amplitude and phase measurement can be greatly simplified if excitation frequency is known: only amplitude and phase estimation is needed then. We suggest the sine wave correlation (SWC) to extract the signal amplitude and phase from the acquired data set [14]. The use of sine-fitting techniques can largely reduce the influence of a noise in final results [9]. If we use the same reference frequency for DDS used to generate the exciting signal and the acquisition ADC, the more simple form of sine-fitting can be used. Then the wave to be fit is defined as:

$$v(t) = V_I \cos(2\pi ft) + V_Q \sin(2\pi ft) + V_0, \qquad (1)$$

where V_I and V_Q are the in-quadrature amplitudes of the sine wave, V_0 is the DC component and f is the excitation frequency used. Fitting this function to the set of N samples, $s_1 \ldots s_N$, acquired at a frequency f_s at time instances $t_1 \ldots t_N$, is accomplished by seeking the minimum of approximation error root-mean-square (RMS) value:

$$\varepsilon_{RMS} = \sqrt{\frac{1}{N}\sum_{n=1}^{N}\left\{s_n - \left[V_I \cos(2\pi ft_n) + V_Q \sin(2\pi ft_n) + V_0\right]\right\}^2} \qquad (2)$$

The procedure is simple and iterative, thus consuming a lot of a computational time. The other approach could be to use a non-iterative procedure: closer look at the operations performed indicate the similarity of the operations performed to a correlation procedure, inherent in the Fourier transform. Therefore the procedure can be presented in a simplified way which is more computational efficient: as correlation coefficient of sine and cosine with sampled version of s_n windowed by some window w_n and normalized by L1 norm $|W|_1$ of the window:

$$V_I(f) = \frac{2\sum_{n=0}^{N-1}\left[\cos(2\pi ft_n)\cdot s_n \cdot w_n\right]}{N|W|_1},$$

$$V_Q(f) = \frac{2\sum_{n=0}^{N-1}\left[\sin(2\pi ft_n)\cdot s_n \cdot w_n\right]}{N|W|_1}, \qquad (3)$$

$$V_0(f) = \frac{2\sum_{n=0}^{N-1} s_n}{N}.$$

Then magnitude and phase of the measured signal is estimated as:

$$V_m(f) = \sqrt{V_I(f)^2 + V_Q(f)^2},$$
$$\varphi(f) = \arctan\left(\frac{V_Q(f)}{V_I(f)}\right). \quad (4)$$

Frequency mismatch induced errors reduction can be obtained.

If additive white Gaussian noise (AWGN) with amplitude V_{nRMS} is present over first Nyquist zone f_{N} at sampling frequency f_{s} then corresponding noise voltage density is [14]

$$VSD_n = \frac{V_{nRMS}}{\sqrt{f_N}} = \frac{V_{nRMS}\sqrt{2}}{\sqrt{f_s}}. \quad (5)$$

Application of SWC on signal array of length N will produce frequency bin f_s/N wide. The standard deviation $\sigma(\mathrm{V_m})$ of the amplitude estimated using (3) and (4) will be [14].

$$\sigma(V_m) = \frac{V_{nRMS}}{\sqrt{N}}\sqrt{2}. \quad (6)$$

The ADC quantization errors can be accounted using ADC full scale voltage V_{FS} and quantization bits number K:

$$V_{ADCnRMS} = \frac{V_{FS}}{2^K\sqrt{12}}. \quad (7)$$

Then for 10 bit ADC it will correspond to 40 nV/√Hz compared to 1.4 nV/√Hz Johnson noise voltage density of 50 Ω source [1]. With all noise sources accounted (6) yields 50 μV expanded uncertainty [1]. Experiments carried out with the developed system indicated 78 μV standard deviation.

3. System Structure

To ensure system universality, system parameters have to be chosen to match the measurement tasks planned [1]. System (Fig. 1) is composed from control part (both local and remote PC can be used), excitation signal generator and the signals acquisition units. Modular construction has been chosen. Industrial standard PC104 is used as form factors and bus. The excitation channel and the receiving channels are connected to the device under test (DUT) via alternative modules according to the measurement task.

In case of remote host, connectivity and control is accomplished by separate PCB in a stack, using the Cypress Semiconductor Corporation's EZ-USB FX2LP IC CY7C68013A. It is a highly integrated, low-power USB2.0 microcontroller, incorporating the USB2.0 transceiver, serial interface engine, local semaphore microcontroller and a programmable peripheral interface (GPIF). The GPIF is programmed as a bridge to the PC104 bus.

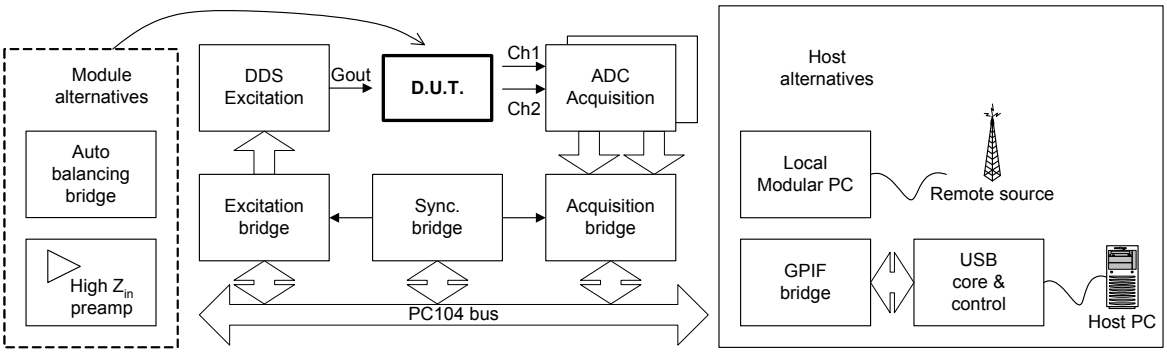

Fig. 1. Acquisition system structure.

4. Synchronization Bus Structure

System is using the direct-digital-synthesis (DDS) based excitation signal generator and two simultaneous 10 bit analog-to-digit converters (ADC) for resulting waveforms collection. The clock frequency of the excitation and reception channels has to be derived from the same clock source in order to allow the SWC use. Acquisition timing is implemented for case when several (more than two) ADC channels are required, or dedicated arbitrary waveform generator is used for applications demanding short dwell time. Full synchronization structure is presented in Fig. 2.

Acquisition timing is accomplished by 25 MHz system clock, which is derived from main 100 MHz

100 ppm 5 ps jitter clock. Acquisition is triggered by St/Sp signal. The DDS generator is deriving its clock by multiplication of the system clock by 6.

5. Excitation Channel Structure

The excitation channel consists of three major components: DDS generator, implemented as AD9851 from Analog Devices [15], gain block based on AD8055 and output attenuator (Fig. 3).

The phase accumulator performs an integration function and generates a linear phase "ramp" in proportion to the desired frequency. The sine lookup table converts the linear phase ramp into a sine wave. Even though the AD9851 contains a 32 bit frequency control register, a 32 bit (232 memory bits) lookup table is not required, as it only has a 10 bit DAC [15]. The output signal after filtering and amplification can be attenuated by smooth attenuator and two stages of 20 dB step attenuators connected in series. The DDS control is accomplished by PC from PC104 bus accessible via M4A3-64/32 bridge CPLD from USB interface or by local host PC in PC104 form factor.

6. Reception Channels Structure

The other most important unit is the receiving channel (Fig. 4). It consists of the optional blocks (high impedance preamplifier, impedance measurement front-end or input attenuator) and the two channels ADC. The high speed dual channel data acquisition consists of the two high speeds ADCs AD9214. The AD9214 is a low power 10 bit monolithic sampling ADC with an on-chip track-and-hold and reference circuits. It is operated at 100 MS/s conversion rate.

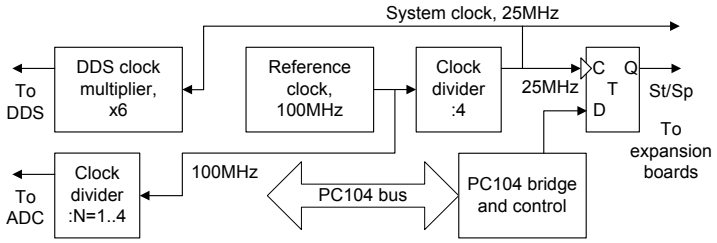

Fig. 2. Synchronization bus structure.

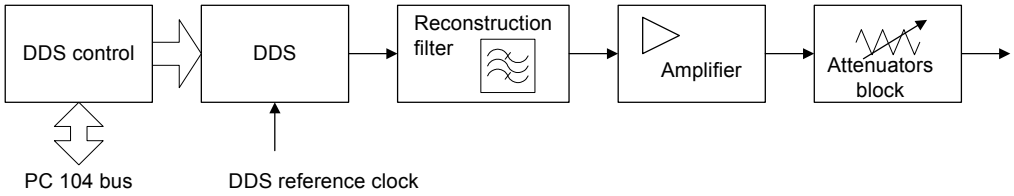

Fig. 3. Excitation channel structure.

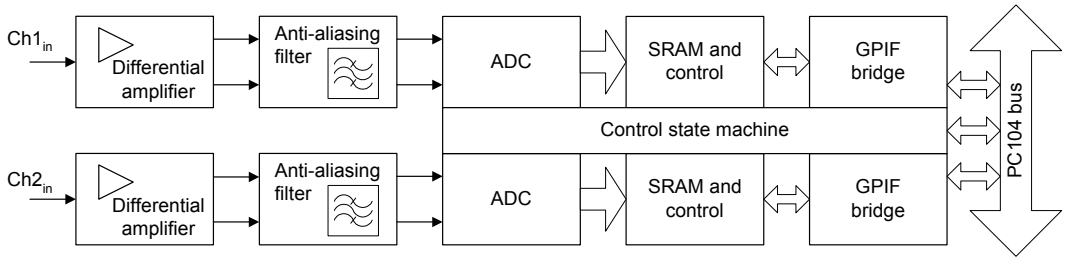

Fig. 4. Reception channel structure.

To sustain the 100 MS/s data transfer rate the ADC conversion result is streamed to the high speed buffer SRAM IS61LV25616 from Integrated Silicon Solution, Inc. The ISSI IS61LV25616 is a high-speed (address access time is 8 ns), low power, 4 Mbit static RAM organized as 256 k words by 16 bits. All the intermediate latching, synchronization and control of the fast 100 MHz clock frequency acquisition state machine is organized by M4A3-128/64 VC-7 CPLDs. The CPLD also performs the PC104 bridge functions. The rest of control is also accomplished via a local PC104 form-factor host computer or by using the GPIF bridge delivered via USB interface.

7. Application Examples

Acquisition module PC-104 stack photo is presented in Fig. 5.

The top PCB is the excitation DDS with optional RMS detector channel. Middle PCB is the dual channel ADC card. The bottom card is the USB interface and PC104 bridge board. Impedance measurement module, incorporating the auto balancing bridge (ABB) circuitry is visible in the lower right corner.

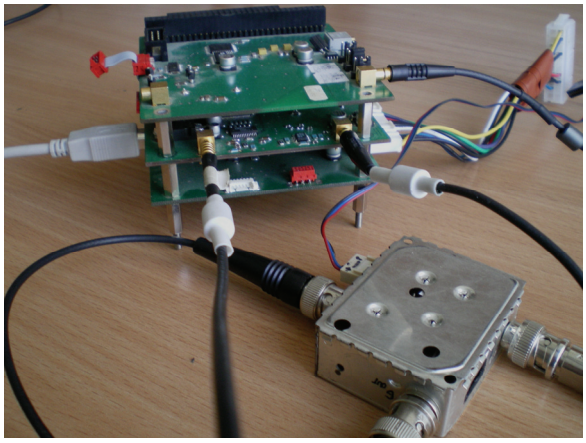

Fig. 5. Acquisition system setup example for impedance measurement.

It can be expected that the DDS output voltage is stable over the designed frequency range. But due to phase rounding inherent to the DDS output, the signal has a slight variation in amplitude related to the output frequency. This is only the case at frequencies close to the half of the reference clock (100 MHz). Also the cables and output impedance introduce the discrepancies in the output amplitude at mismatched loads. These can be accounted as system insertion losses and stored in a computer memory as compensation coefficient. Various measurement tasks can be performed using the system developed.

7.1. Ultrasound Transmission Evaluation

The frequency response of device under test (DUT) at certain frequency can be determined by probing the system input with a single frequency sine signal while measuring the input and the output signal voltages $u_{in}(f)$ and $u_{out}(f)$ the preamplifier response is given by:

$$G(f)=\frac{u_{out}(f)}{u_{in}(f)}\cdot k(f), \tag{8}$$

where $k(f)$ is used for cables and output impedance influence compensation. All the measurements presented below did not use this compensation. The gain AC response of ultrasonic preamplifier is presented in Fig. 6 a. Ultrasound transmission in liquids was investigated in similar way (Fig. 7).

Two wideband transducers TF5C6 from Guangzhou Doppler Electronic Technologies were used. Transducers were placed on opposite ends of 8 mm diameter and 85 mm long measurement channel filled with liquid. Water and ethanol were used for investigation. Harmonic CW excitation signal was applied on transmitting transducer. Same signal was routed back to ADC input 1. The opposite transducer's output was supplied to ADC input 2. This way both excitation and reception voltage was recorded. The transmission response was obtained using (3) and (8). Obtained magnitude response is presented in Fig. 6 b.

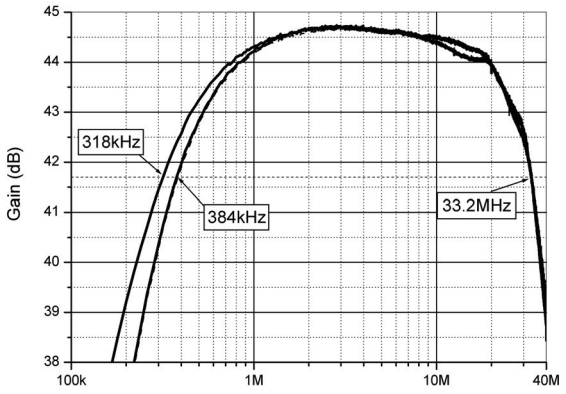

(a)

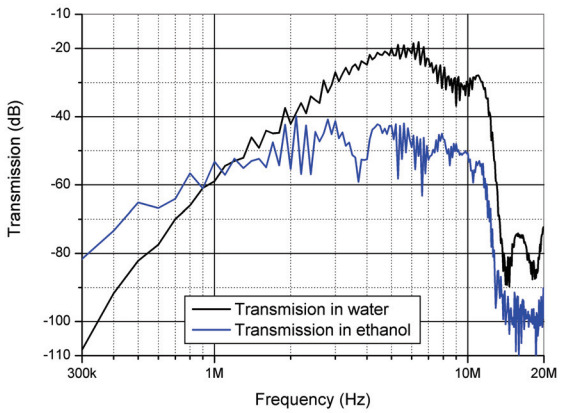

(b)

Fig. 6. Transmission AC response for: a) ultrasonic preamplifier and b) ultrasound transmission in liquids.

Investigation indicates that attenuation in ethanol is up to 30 dB higher than in water. The AC response ripple was produced by CW signal interference in measurement channel. Measurement results were used to predict the signal transmission level in ultrasonic transit time flow meter design. Such measurement useful in the ultrasonic transducer design phase: changes in transmission can be monitored for coupling layers or backing influence.

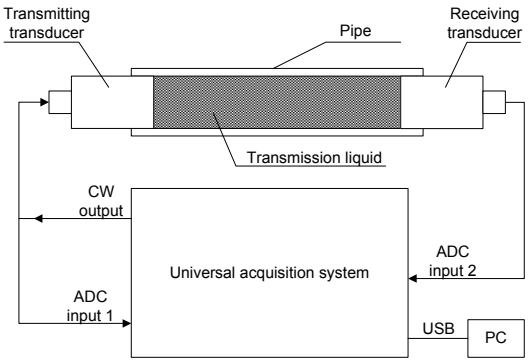

(a)

(b)

Fig. 7. Transmission AC response measurement a) setup and b) chamber photo.

7.2. Signal Distortion Measurement

In case of nonlinear or parametric circuit presence new frequency components appear at the DUT output. Total Harmonic Distortion (THD) is a most common measure of an amplifier distortions specification [16]. It compares the power of harmonics V_2 to V_k with the total signal power:

$$THD = 10\log_{10}\left(\frac{\sum_{k=2}^{K} V_k^2}{\sum_{k=1}^{K} V_k^2}\right), \quad (9)$$

Wideband ultrasonic preamplifier output signal harmonic distortion was analyzed. Analysis was carried out using the Agilent N9320A spectrum analyzer (resolution bandwidth 3 kHz) and the designed acquisition system. CW 1MHz signal from acquisition system was supplied to preamplifier input. Gain of preamplifier was set to 45 dB. Amplifier output was recorded 100 times using 100 MHz sampling and 32 k samples record length. In order to compare the windowing performance, rectangular window (no window), Hamming window and truncation was used on acquired data. Every record obtained was converted to frequency domain using FFT. Then results were converted to power spectrum, averaged power-wise and converted to RMS value. Same data was used to obtain harmonics amplitudes using SWC and converted to RMS (Fig. 8).

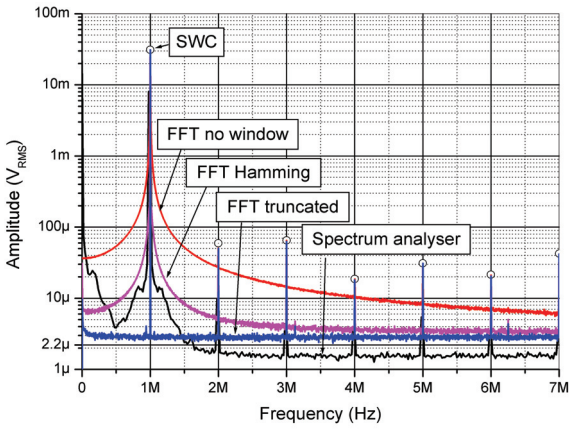

(a)

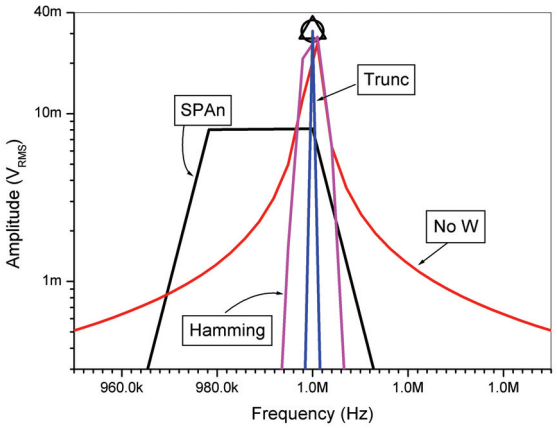

(b)

Fig. 8. Harmonics distortion measurement results: a) 6 harmonics span and b) zoomed first harmonic.

It can be seen that the truncated version has the best performance in spectrum estimation. Unfortunately, all FFT-based techniques have than spectrum analyzer higher noise floor due to 10 bits ADC – approximately 2.2 μV. Spectrum analyzer data was approximated to fit into limited number of points per frequency range, therefore spectral accuracy was lost. It was possible to obtain similar to SWC results on spectrum analyzer, but only at significant zoom. SWC data was used to obtain the total harmonic distortion: TDH = -49 dB was obtained with rectangular window and -50 dB with truncation.

7.3. Ultrasonic Transducer Impedance Measurement

The circuit impedance is an important parameter characterizing the electronic circuits, components, and the materials. To find the impedance, one needs to measure at least two values because of its complexity. Modern impedance measuring instruments measure the real and the imaginary parts

of an impedance vector and then convert them into the desired parameters [17].

A variety of measurement methods for impedance measurement exists [17]. System is using the auto-balancing bridge (ABB) technique for impedance measurement. The measured impedance Z_x can be calculated using Ohm's law from the voltage and current values. The ABB technique employs the inverting topology operational amplifier (Fig. 9).

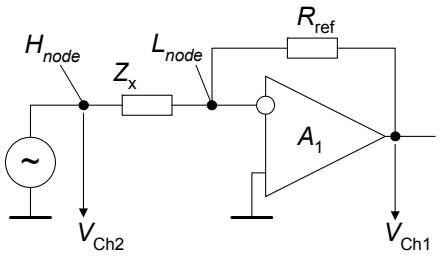

Fig. 9. Acquisition system setup example for impedance measurement.

The current flowing through Z_x is mirrored by the resistor R_{ref} current. The potential at the operational amplifier inverting pin is maintained at zero (sometimes called a "virtual ground"). Then the output voltage (measured by ADC Ch1, V_{Ch1}) of the operational amplifier is in direct proportion to the current flowing in Z_x. The Z_x can be obtained as:

$$Z_x = \frac{V_{Zx}}{I_{Zx}} = \frac{V_{Ch2}}{V_{Ch1}} R_{\text{ref}}, \tag{10}$$

Results of ultrasonic transducer impedance measurements carried out using our system and precision impedance analyzer 65120B from Wayne Kerr Electronics [18] are presented in Fig. 10.

Fig. 10 results indicate that system has acceptable performance in impedance evaluation. Thanks to high SNR obtained system allows to carry out majority of impedance measurements without the change of the reference resistor R_{ref}. All the results presented have been obtained using 2 kΩ reference resistor.

A true value is the value of an ideally packaged circuit component. The effective value takes into consideration the effects of a component's parasitic. The indicated value is the value obtained with the measurement instrument. It includes the instrument's inherent losses and inaccuracies. Indicated values always contain errors when compared to true or effective values. They depend on a multitude of considerations. By comparing how close the indicated value agrees with the effective value allow to asses the measurement quality. In other words, the goal of measurement is to have the indicated value to be as close as possible to the effective value. The implementation of the remote measurements requires the connections for signal routing [19].

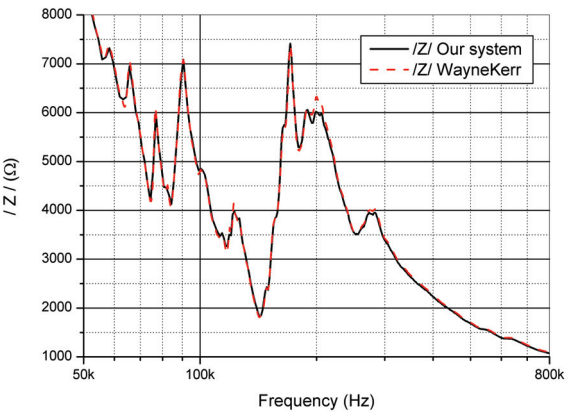

(a)

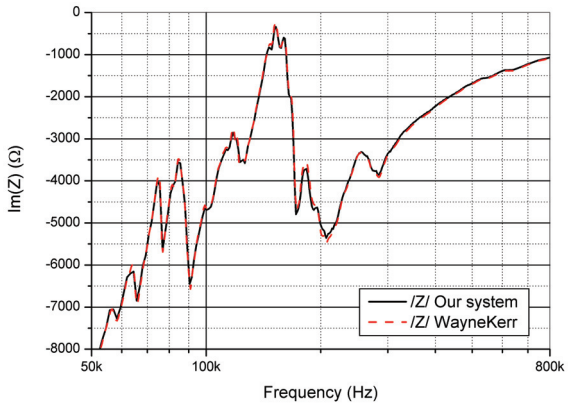

(b)

Fig. 10. Ultrasonic transducer measurement results: a) impedance magnitude and b) imaginary part.

The imperfectness of the measurement circuit is compensated using the software compensation by application of the additional Open/Short/Load measurement results [20]:

$$Z_{DUT} = Z_{std} \frac{(Z_o - Z_{stdm}) \cdot (Z_{xm} - Z_s)}{(Z_{stdm} - Z_s) \cdot (Z_o - Z_{xm})}, \tag{11}$$

where Z_{xm} is the measured DUT impedance; Z_s and Z_o are the measured impedance values when routing connections are shorted and open accordingly; Z_{stdm} and Z_{std} are the measured and theoretical impedance values of some standard device with a known impedance value. Values are stored in computer memory and later used for succeeding measurements compensation.

Examples of ultrasonic actuator impedance monitoring application are presented in Fig. 11. Here, impedance change with actuator load and excitation signal value is presented.

In first example, the ultrasonic actuator dedicated for micro-motor application was examined under different load conditions: i) no coupling to rotation shaft and ii) coupling to rotation shaft. Experimental results of complex impedance measurement are

presented in Fig. 11 a. Another example presents the influence of the different excitation voltage levels in obtained impedance. Excitation generator voltages of 40 V and 4 V were applied. Experimental results of complex impedance measurement are presented in Fig. 11 b.

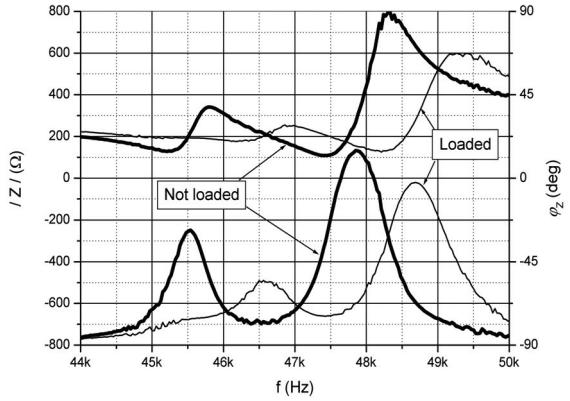

(a)

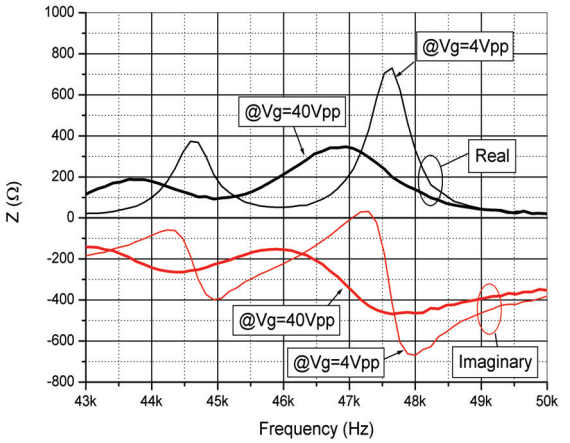

(b)

Fig. 11. Monitoring of the ultrasonic actuator impedance change (a) by loading; (b) by excitation voltage.

7.4. Ultrasonic Transducer Impedance Measurement for Power Delivery Estimation

Ultrasonic transducer impedance measurement results can be used to estimate the transducer excitation efficiency or to calculate the electrical matching circuits [21, 22]. Power delivery to load is maximized when load impedance is equal to generator intrinsic resistance R_g. In case of complex load impedance the imaginary part (Fig. 10) is reducing the efficiency of the electrical power conversion the pressure wave. These parameters can be modified by applying the electrical circuit in between the ultrasonic transducer and excitation generator [7, 24]. With the measured transducer impedance available, transducer performance can be estimated without the need for model derivation. Example of air coupled transducer evaluation for matching circuit influence is presented in Fig. 12.

Unmatched transducer was not able to efficiently operate at 900 kHz. After application of inductor imaginary part of the impedance at 900 kHz frequency was reduced. Two circuits were used: with inductor connected in series and inductor connected in parallel to transducer contacts. Parallel compensating inductor value L_{par} can be calculated using measured transducer impedance Z_T:

$$L_{par} = -\frac{X_{par}\big|_{\omega=\omega_s}}{\omega_s},$$

$$X_{par} = \mathrm{Im}(Z_T)\frac{\left[1+\left(\frac{\mathrm{Im}(Z_T)}{\mathrm{Re}(Z_T)}\right)^2\right]}{\left(\frac{\mathrm{Im}(Z_T)}{\mathrm{Re}(Z_T)}\right)^2}, \quad (12)$$

$$R_{par} = \mathrm{Re}(Z_T)\left[1+\left(\frac{\mathrm{Im}(Z_T)}{\mathrm{Re}(Z_T)}\right)^2\right]$$

Serial compensating inductor value L_{par} can be calculated as:

$$L_{ser} = \frac{\mathrm{Im}(Z_T)}{\omega_s}. \quad (13)$$

More details on ultrasonic transducer matching circuits can be found in [23].

Graphs in Fig. 12 are of little use since there is no evident advantage of any matching technique. Quantitative matching performance evaluation criteria have been suggested in [24]: i) Power delivered to load at operation frequency; ii) -3 dB bandwidth; iii) Effective bandwidth; iv) Power delivery to load efficiency; v) Power factor and vi) Total efficiency. Here we only concentrate on power delivery efficiency.

Measured transducer impedance can be used to calculate the complex power delivered to it:

$$S_T = \frac{e_g^2 Z_{in}}{\left(R_g + Z_{in}\right)\left(R_g + Z_{in}^*\right)}, \quad (14)$$

where e_g is the intrinsic generator voltage; Z_{in} is the transducer input impedance (if matching circuit is applied in between) and R_g is the generator intrinsic resistance. Assuming that losses in matching circuit are negligible then real part P_T of the complex power S_T is equal to the power dissipated in transducer. In case of optimal transducer design it can be further assumed that this power is in direct proportion to the acoustic emission of the transducer [25]. Then the power delivery to load efficiency criteria can be

established, which establishes the ratio of the real power conveyed to load and the power available from generator [24]:

$$\eta = \frac{4R_g \operatorname{Re}(S_T)}{e_g^2} 100\% = \frac{4R_g Z_{in}}{(R_g + Z_{in})(R_g + Z_{in}^*)} 100\% \quad (15)$$

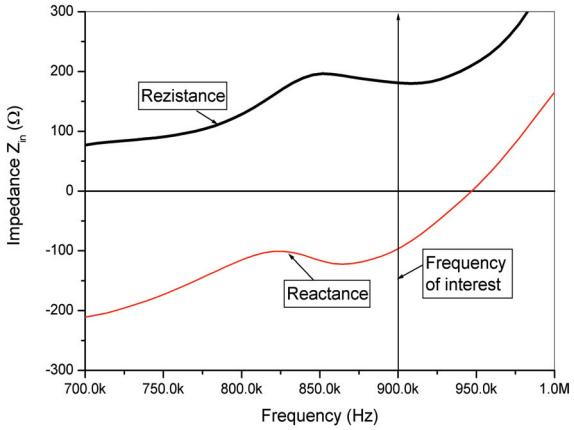

(a)

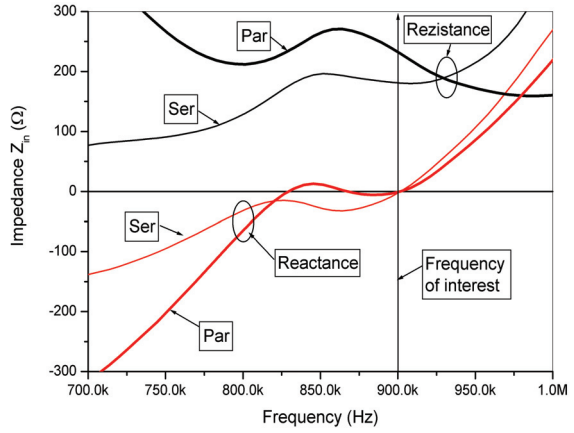

(b)

Fig. 12. Ultrasonic transducer impedance matching: (a) original, (b) after series and parallel inductance application.

The results of power delivery efficiency investigation are presented in Fig. 13. Transducer impedance was measured and "L" matching [26] circuit application influence on impedance obtained (Fig. 13 a). Power delivery efficiency was calculated for two matching circuits: with impedance matching at 11 MHz and at 5 MHz (Fig. 13 b).

Analysis of the power delivery efficiency graph above indicates that same matching technique gives different results: in some case passband is improved (matching at 11 MHz) but another condition (different matching frequency, 5 MHz) has much narrower bandwidth. Availability of impedance for analysis allows to fine tune the matching circuit for optimum performance.

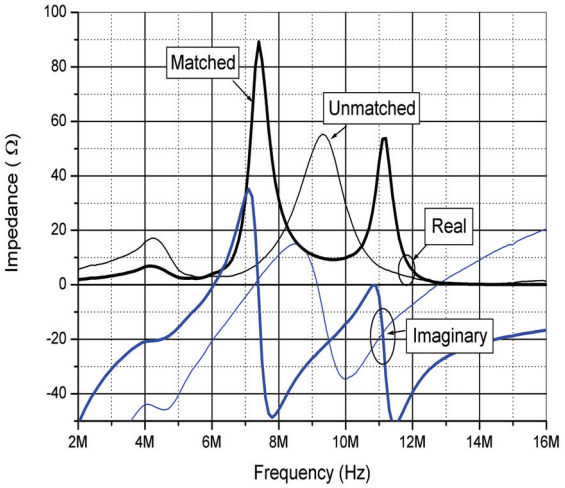

(a)

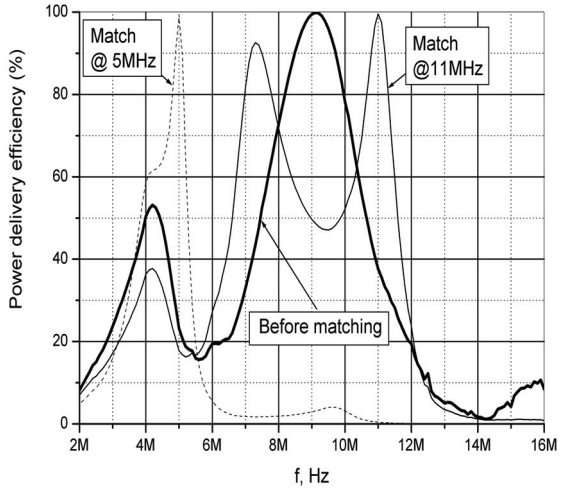

(b)

Fig. 13. Ultrasonic transducer impedance "L" matching (a) influence on power delivery efficiency (b).

7.5 Ultrasonic Transducer and Preamplifier Combined Noise Performance Investigation

The preamplifier output noise density can be obtained by modeling the amplifier intrinsic noise using voltage source e_n and current noise sources i_{n+} and i_{n-} [27]. Simplified ultrasonic preamplifier structure, realized using operation amplifier is presented in Fig. 14.

Measured transducer impedance Z_T can be used for total output noise estimation:

$$e_{ntot}^2 = G^2 \left| \frac{R_t}{R_t + Z_T} \right|^2 e_s^2 + G^2 \left| \frac{Z_T}{R_t + Z_T} \right|^2 e_t^2 + \\ + G^2 \left| \frac{R_t Z_T}{R_t + Z_T} \right|^2 i_{n+}^2 + G^2 e_n^2 + (G-1)^2 e_1^2 + e_2^2 + R_2^2 i_{n-}^2 \quad (16)$$

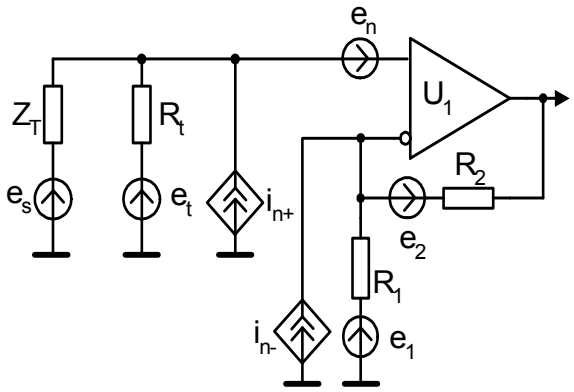

Fig. 14. Combined ultrasonic transducer and preamplifier noise model circuit.

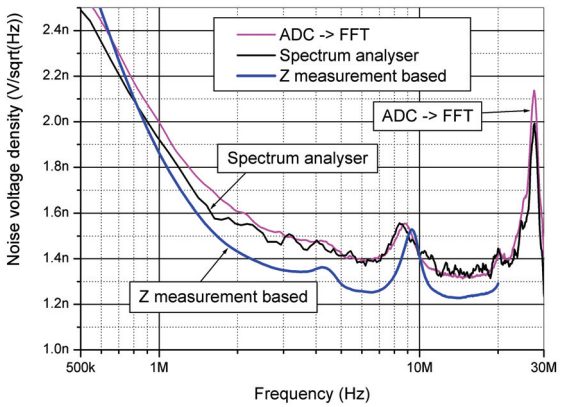

Fig. 15. Ultrasonic transducer and preamplifier combined input-referred noise voltage density estimation.

where e_t is the noise spectral density of the input biasing resistance R_t, e_t^2 is noise power spectral density and G is the amplifier gain

$$e_t^2 = 4kTR_t, \tag{17}$$

with k=1.380658·10^{-23} J/C - Bolzmann constant, T is the absolute ambient temperature; e_s is the noise component of the ultrasonic transducer with complex impedance Z_T

$$e_s^2 = 4kT\,\mathrm{Re}(Z_T), \tag{18}$$

The feedback circuit contributes as

$$e_1^2 = 4kTR_1;\ e_2^2 = 4kTR_2. \tag{19}$$

For the input-referred noise it can be simplified into three main components: source thermal noise e_s, amplifier input voltage source noise e_n and current source noise:

$$VSD_n^2 = e_s^2 + e_n^2 + |Z_T|^2 i_{n+}^2. \tag{20}$$

Then, impedance measurement results can be used for ultrasonic transducer and preamplifier combined noise estimation [3-6, 28]. Fig. 15 is used to compare the noise estimation using the source impedance measurement and conventional noise estimation using Agilent N9320A spectrum analyzer.

It is worth to note out that our acquisition system is capable to record the signals from the DUT with sufficient record length (32 k or even 256 k samples long). If DUT output is passed through low noise amplifier with flat frequency response and known gain value, these measurements can be used noise spectral density estimation. Here, FFT can be used for noise power spectrum estimation. Then multiple noise power density measurements can be power-wise averaged C_{max} times to obtain the statistical noise estimate.

$$PSD = \frac{2\sum_{c=1}^{C_{max}}\left|\sum_{n=0}^{N-1} s_n e^{-i\frac{2\pi}{N}nk}\right|^2}{f_s C_{max} N}. \tag{21}$$

Noise level measurement using the Agilent N9320A spectrum analyzer and the designed system comparison was carried out. Record length of 32 k samples is equivalent to 3 kHz resolution bandwidth of spectrum analyzer: such condition was used in measurements. Amplifier output noise was recorded C_{max}=1000 times. Every record obtained was converted to frequency domain using Fourier transform. Rectangular window was used on acquired data. Then results were converted to power spectrum, averaged and power spectral density obtained (Fig. 14). Then, using quite simple acquisition system amplifier noise performance can be estimated both using transducer impedance measurement results and both multiple records of output noise and Fourier analysis.

8. Conclusions

Structure and design approach of the versatile signals acquisition system for ultrasonic equipment parameters estimation has been presented. The modular architecture of the system allows for both local and remote PC connectivity. Setup and results for system application examples and measurement results are presented. System allows measuring multiple frequency domain parameters measurement using just two ADC channels and DDS generator. Thanks to the inherent processing gain of the sine wave correlation technique, large dynamic range of vector voltage measurement is obtained using just 10 bit ADC. Operation range is 20 kHz to 30 MHz. Transfer AC response, insertion loss, harmonic distortions, noise and electrical impedance measurement results indicate that system has acceptable performance. High SNR and large

dynamic range allow performing the majority of ultrasonic transducers impedance measurements without the need to change the reference resistor. Comparison with benchtop impedance analyzer 65120B from Wayne Kerr Electronics indicates the acceptable device performance in impedance estimation. Availability of impedance for analysis allows to fine tune the matching circuit for optimum performance. Ultrasonic equipment noise estimation can be carried out. Amplifier noise performance can be estimated both using transducer impedance measurement results and both multiple records of output noise and Fourier analysis. Noise measurement results were compared against results obtained by Agilent N9320A spectrum analyzer. Comparison indicated acceptable noise estimation performance.

Acknowledgements

This research was funded by a grant (No. MIP-058/2012) from the Research Council of Lithuania.

References

[1]. L. Svilainis, V. Dumbrava, A. Chaziachmetovas, Universal acquisition system for frequency domain parameters measurement, in *Proceedings of 6th IEEE International Conference on Intelligent Data Acquisition and Advanced Computing Systems (IDAACS'2011)*, 2011, pp.10-15.

[2]. M. Garcia-Rodriguez, et al., Low cost matching network for ultrasonic transducers, *Physics Procedia*, Vol. 3, Issue 1, January 1, 2010, pp. 1025-1031.

[3]. L. Svilainis, V. Dumbrava, A. Chaziachmetovas, Ultrasonic preamplifier performance evaluation, in *Proceedings of IEEE Conference on Information Technology Interfaces*, June 21-24, 2010, pp. 663-668.

[4]. A. Turo, J. Salazar, J. A. Chavez, et al., Ultra-low noise front-end electronics for air-coupled ultrasonic non-destructive evaluation, *NDT&E International*, Vol. 36, 2003, pp. 93-100.

[5]. V. Dumbrava, L. Svilainis, Noise model for ultrasonics transducer preamplifier, *Electronics and Electrical Engineering,* Vol. 66, 2006, pp. 62-66.

[6]. T. L. Rhyne, Characterizing ultrasonic transducers using radiation efficiency and reception noise figure, *IEEE Transactions UFFC*, Vol. 45, 1998, pp. 559-566.

[7]. J. Emeterio, A. Ramos, P. Sanz, A. Ruiz, Evaluation of impedance matching schemes for pulse-echo ultrasonic piezoelectric transducers, *Ferroelectrics*, Vol. 273, Issue 1, 2002, pp. 297-302.

[8]. V. Haasz, AXIe – new standard for the highest performance test and measurement applications, in *Proceedings of 6th IEEE International Conference on Intelligent Data Acquisition and Advanced Computing Systems (IDAACS'2011)*, 2011, pp. 30-32.

[9]. M. Silva, P. M. Ramos and A. C. Serra, A new four parameter sine fitting procedure, *Measurement*, Vol. 35, 2004, pp. 131-137.

[10]. G. Heinzel, A. Rudiger and R. Schilling, Spectrum and spectral density estimation by the discrete Fourier transform (DFT), including a comprehensive list of window functions and some new at-top windows, *Report. Max-Planck-Institut fur Gravitationsphysik*, Hannover, February 15, 2002.

[11]. D. Bellan, Real-time detection of sine waves by means of a discrete Fourier transform, in *Proceedings of 5th IEEE International Workshop on Intelligent Data Acquisition and Advanced Computing Systems (IDAACS'2009)* 2009, pp. 458-461.

[12]. T. Li, Y. Tang and J. Lv., Parameter estimation of FH signals based on STFT and music algorithm, in *Proceedings of IEEE Conference on Computer Application and System Modeling*, Vol. 5, October 2010, pp. V5-232.

[13]. M. Tsuji, S. Hamasaki, and M. Korogi, Characteristics of power series type wavelet transform for online frequency estimation, in *Proceedings of Power Conversion Conference*, April, 2007, pp. 177-182.

[14]. V. Dumbrava, L. Svilainis, The automated complex impedance measurement system, *Electronics and Electrical Engineering*, Vol. 76, 2007, pp. 59-62.

[15]. CMOS 180 MHz DDS/DAC Synthesizer AD9851, Data sheet revue D, *Analog Devices, Inc.*, 2004.

[16]. S. Temme, Audio distortion measurements, Application note, *Bruel and Kjer*, 1997.

[17]. Eight hints for successful impedance measurements, Application Note 346-4, *Agilent Technologies*, 2000.

[18]. Precision Impedance Analyzers 6500B Series, *Wayne Kerr Electronics*, London, 2011, (http://www.waynekerrtest.com/global/html/products/impedance analysis/6500.htm).

[19]. L. Svilainis, V. Dumbrava, Test fixture compensation techniques in impedance analysis, *Electronics and Electrical Engineering*, Vol. 87, Issue 7, 2008, pp. 37-40.

[20]. Effective impedance measurement using open/short/load correction, Application Note 346-3*, Agilent Technologies*, 1998.

[21]. A. Ramos, J. Emeterio, P. T. Sanz, Dependence of pulser driving responses on electrical and motional characteristics of NDE ultrasonic probes, *Ultrasonics*, Vol. 38, 2000, pp. 553-558.

[22]. R. Thurston, Effect of electrical and mechanical terminating resistances on loss and bandwidth according to the conventional equivalent circuit of a piezoelectric transducer, *IRE Transactions on Ultrasonic Engineering*, 1960, pp. 16-25.

[23]. L. Capineri, L. Masotti, M. Rinieri and S. Rocchi, Ultrasonic transducer as a black-box: equivalent circuit synthesis and matching network design, *IEEE Transactions on Ultrasonics, Ferroelectrics and Frequency Control*, Vol. 40, 1993, pp. 694-703.

[24]. L. Svilainis, V. Dumbrava, Evaluation of the ultrasonic transducer electrical matching performance, *Ultrasound*, Vol. 62, 2007, pp. 16-21.

[25]. V. Khmelev, I. Savin et. al., Problems of electrical matching of electronic ultrasound frequency generators and electro acoustical transducers for ultrasound technological installations, in *Proceedings of 5th International Siberian Workshop and Tutorial*, 2004, pp. 211-215.

[26]. G. Petersen, L-matching the output of a RITEC gated amplifier to an arbitrary load, Application note, *RITEC Inc.*, USA. 2006.

[27]. C. D. Motchenbacher, J. A. Connelly, Low noise electronic system design, *John Willey & Sons Inc*., 1993.

[28]. W. M. Leach, Noise analysis of transformer-coupled preamplifiers, *Journal of Audio Engineering Society*, Vol. 40, 1992, pp. 3-11.
